Hydrogen-induced anomalous Hall effect in Co-doped ZnO

2014 New J. Phys. 16 073030

(http://iopscience.iop.org/1367-2630/16/7/073030)

New Journal of Physics
The open access journal at the forefront of physics
Deutsche Physikalische Gesellschaft DPG | IOP Institute of Physics

Hydrogen-induced anomalous Hall effect in Co-doped ZnO

Yong Chan Cho[1], Seunghun Lee[2], Ji Hun Park[3], Won Kyoung Kim[3], Ho-Hyun Nahm[4], Chul Hong Park[5] and Se-Young Jeong[1,3]

[1] Crystal Bank Institute, Pusan National University, Miryang 627–706, Korea
[2] The Institute of Basic Science, Korea University, Seoul 136–701, Korea
[3] Department of Cogno-Mechatronics Engineering, Pusan National University, Miryang 627–706, Korea
[4] Center for Correlated Electron Systems, Institute for Basic Science (IBS) & Department of Physics and Astronomy, Seoul National University, Seoul 151–747, Korea
[5] Department of Physics Education, Pusan National University, Busan 609–735, Korea
E-mail: syjeong@pusan.ac.kr

Received 7 April 2014, revised 10 June 2014
Accepted for publication 24 June 2014
Published 22 July 2014

New Journal of Physics **16** (2014) 073030
doi:10.1088/1367-2630/16/7/073030

Abstract

The electrical transport characteristics and anomalous Hall effect (AHE) were investigated for a hydrogen-injected Co-doped ZnO thin film. Based on the measurements of resistivity and the Hall effect between 5 K and 300 K, the existence of Co-H-Co complexes was observed to introduce the AHE and enable the AHE to persist up to room temperature. The observed H-induced AHE originates from the asymmetric scattering of carrier hopping between the localized states driven by ferromagnetic Co-H-Co complexes, and a theoretical study using first-principle calculations supports the experimental results well. This large ferromagnetic response of charge carriers by the hydrogen-induced AHE on semiconducting oxides will stimulate the further investigation of room-temperature spintronic applications.

Keywords: anomalous Hall effect, hydrogen mediated ferromagnetism, Co-doped ZnO

1. Introduction

Ferromagnetic semiconductors have been considered suitable materials for future spintronics due to the beneficial advantage of the strong coupling between their magnetic and electrical transport characteristics [1]. One of the most promising characteristics of ferromagnetic semiconductors is the anomalous Hall effect (AHE), which can provide the electrical manipulation of a ferromagnetically spin-polarized carrier. The AHE signal has also been assumed to be a useful experiment for characterizing the intrinsic ferromagnetism and providing evidence of the presence of a spin-polarized current. For III-V ferromagnetic semiconductors, the electrical-field control of ferromagnetism as well as magnetization reversal and photo-induced ferromagnetism have been achieved using AHE [2–4]. However, the low Curie temperature of group III-V materials, which is far below room temperature, has hindered the realization of spintronic devices that are operable at room temperature.

Since the possibility of room-temperature ferromagnetism was first predicted based on wide-band-gap semiconductors, there have been tremendous research efforts focused on transition-metal-doped II–VI semiconductors [5–7]. Among these materials, Co-doped ZnO has been intensively studied as a promising candidate for room-temperature ferromagnetism. Several experimental results have provided evidence of the intrinsic ferromagnetism of this material; however, the origin of ferromagnetism still remains unclear, and there are controversial arguments about the extrinsic contributions. Recently, it was reported that nano-clusters of magnetic impurities occur due to spinodal nano-decomposition [8, 9]. The nano-clusters are well separated and show super-paramagnetism. However, ferromagnetic behaviour can be observed in the magnetization process at finite temperatures due to the blocking effect [8, 9].

In previous papers, we theoretically and experimentally demonstrated the ferromagnetism in ZnCoO:H originating from the ferromagnetic spin–spin interaction of the Co-H-Co complex [10–14]. We also demonstrated that hydrogen (H)-induced ferromagnetism can be reversible and reproducible by tuning the injected H. Currently, the localized ferromagnetic domain has been observed using anodic aluminium oxide templates and the localized hydrogenation method [15]. Theoretical calculations predict that the macroscopic percolation of ferromagnetic Co-H-Co complex units would result in ferromagnetic long-range ordering exhibited as room-temperature ferromagnetism, which can contribute to the development of spintronic devices that are operable at room temperature [10]. However, the H-injection is simultaneously accompanied by a large change in the electrical characteristics and by the mediation of spin ordering. Therefore, to manipulate the percolation of complexes in ZnCoO:H, it is necessary to investigate the correlations between the changes of electrical transport and magnetic characteristics due to H incorporations.

Here, we report on the clear H-induced AHE and the changes of carrier density (n) and mobility (μ) in Co-doped ZnO thin films with increasing H incorporation from the surface. We also examined the electronic structure of ZnCoO:H using first-principles calculations. Generally, the local density approximation (LDA) is not sufficient to describe the electronic structure of the localized orbitals in the magnetic semiconductors due to the self-interaction effect [16]. Therefore, in this work, we used the LDA+U method, which compensates for the self-interaction. Through the measurements of resistivity and the Hall effect as well as first-principles calculations, we demonstrate that the injected H can increase the characteristic AHE due to the localized states formed by the hybridization between the H-s orbital and the Co-t_2

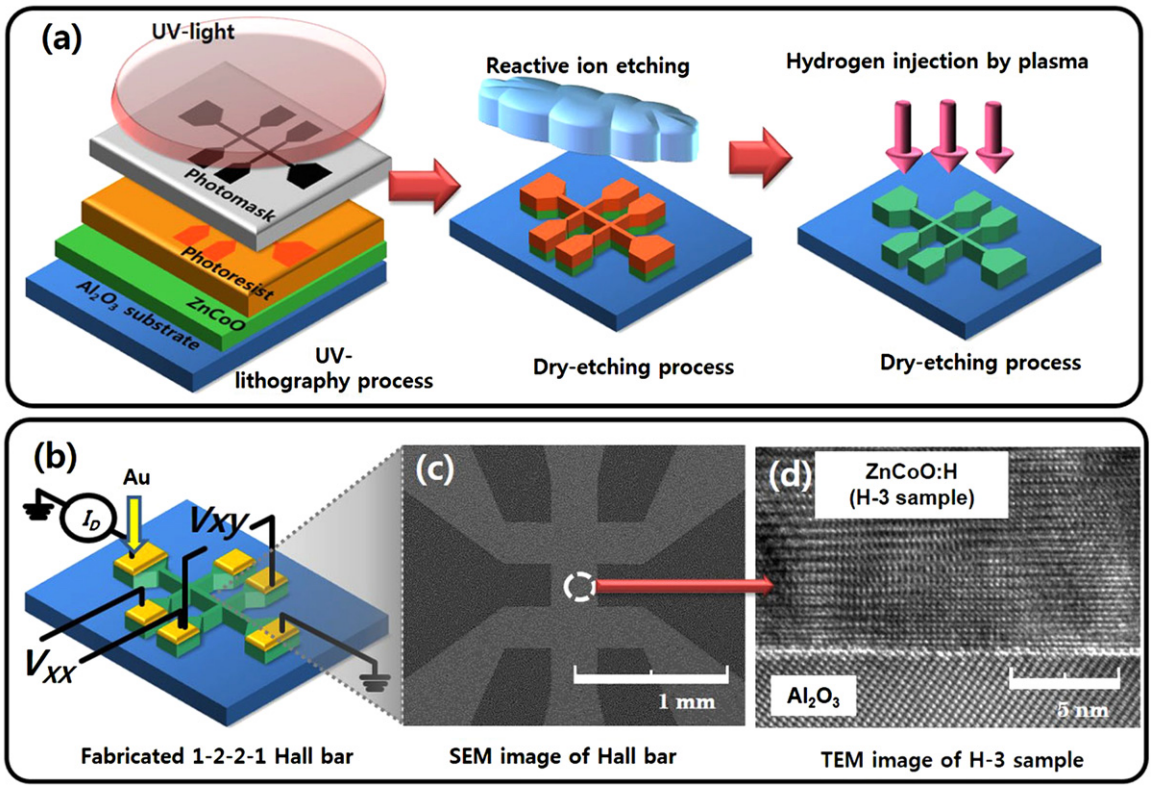

Figure 1. (a) A schematic diagram of the fabrication of the ZnCoO:H Hall bar structure using UV-lithography, reactive ion etching and H-injection. (b) Schematic diagrams for the fabricated 1-2-2-1 Hall bar and measurement. (c) SEM image and (d) HRTEM image of H-3.

orbitals and that unlike other n-type impurities in ZnCoO, the characteristic nature of H can contribute to the formation of ferromagnetic Co-H-Co complexes and to the enhancement of a spin-dependent asymmetric carrier scattering up to room temperature.

2. Experimental

2.1. Sample fabrications

Figure 1(a) presents a schematic diagram for the fabrication of the ZnCoO:H Hall bar structure. Co (10 mol%)-doped ZnO (ZnCoO) thin films were fabricated on Al $_2O_3$(0001) substrates using RF-magnetron sputtering at 350 ^oC. The details of the sample fabrication and measurements are presented and were published in previous studies [11–13]. Six-contact 1–2–2–1 Hall bars with 300–1000 μm channel sizes were fabricated using conventional UV-lithography with photoresist (PR) patterning (figure 1(a)). For this study, the thickness of all samples was fixed at 100 nm. In this study, three different types of ZnCoO:H samples were prepared using different H-injection processes. During the dry-etching process using a reactive ion etcher, H was slightly injected into ZnCoO (H-1 sample). For this H-1 sample, additional H injection processes were performed using RF-plasma with a power of 40 W (H-2 sample) and 80 W (H-3 sample) with an Ar-H_2 (10 wt. %) gas mixture for 10 min. After the H-injection process, the Au

electrode was evaporated on the fabricated Hall bar using DC-sputtering with a shadow mask (figure 1(b)).

As presented in our previous report of the secondary ion mass spectroscopy (SIMS) depth profiles [11], H was uniformly distributed on both the surface and the inside of the hydrogenated sample, but the H concentration was reduced by subsequent vacuum annealing. After vacuum annealing and a second hydrogenation process, the H level was the same as that of the sample inside the film prior to subsequent processing. There was no detectable change in the oxygen level. The H was mainly concentrated 20 nm beneath the surface, and the levels of Zn, Co and O changed at the surface during the second hydrogenation process; these results were not seen in our recent study [13], due to optimized H treatment conditions using HIP.

Figures 1(c) and (d) present scanning electron microscope (SEM) and high resolution transmission electron microscopy (HRTEM) images of the fabricated H-3 Hall bar sample, respectively. Generally, an excessive H treatment can induce extrinsic ferromagnetism such as metal clusters. However, as observed in HRTEM image in figure 1(d), no trace of clustering or a secondary phase was observed, even for the highest plasma power for H-injection (H-3 sample). In our previous and current studies, x-ray absorption spectroscopy and synchrotron x-ray diffraction measurements revealed that the contribution of metallic clusters or crystalline defects is negligible in our optimized H-injection condition [14, 17]. Furthermore, the abnormal magnetic behavior in temperature-dependent magnetization attributed to Co nano-clusters [18] was also not observed for the H-2 or H-3 samples.

2.2. Electrical characterizations and Hall effect measurement

The Au electrode was evaporated on the fabricated Hall bar using DC-sputtering with shadow mask. The transport properties of all the samples were measured by a combinations of a Physical Properties Measurement System (PPMS-9, Quantum Design) with function generator (HP 3325B), Lock-in amplifier (Stanford SR830 DSP) and source meter (Keithley 2425C). The temperature was controlled from 5 to 300 K. After fixing temperature, the magnetic field was slowly swept perpendicular to both the sample surface and current direction between −3 T and 3 T during AHE measurements. In order to minimize the contribution of thermal energy, we measured the transverse and longitudinal voltage with lock-in amplifier during the current (10 μA) reversal (19 Hz). For eliminating any magnetic field effects showing the even function of field, anomalous Hall voltage was obtained by $V(H) = 1/2[V(H) - V(-H)]$. The magnetization was measured as function of temperature by vibrating sample magnetometry (VSM) in PPMS.

3. Results and discussion

3.1. Carrier density(n), mobility(μ) and resistivity(ρ_{xx})

Figure 2(a) shows the temperature dependence of the DC resistivity (ρ_{xx}) and conductivity ($\sigma_{xx} = 1/\rho_{xx}$) (inset figure) as a function of the H incorporation. The as-grown Co-doped ZnO exhibits insulator characteristics (n is almost $10^{15} \sim 10^{16}$ cm^{-3} in our experiment). The H incorporations largely decrease (increase) the ρ_{xx} (σ_{xx}) over the entire temperature region from 5 K to 300 K, indicating that some of the hydrogen should act as the shallow donor. All of the results clearly indicate a negative temperature coefficient of resistivity without any transition to

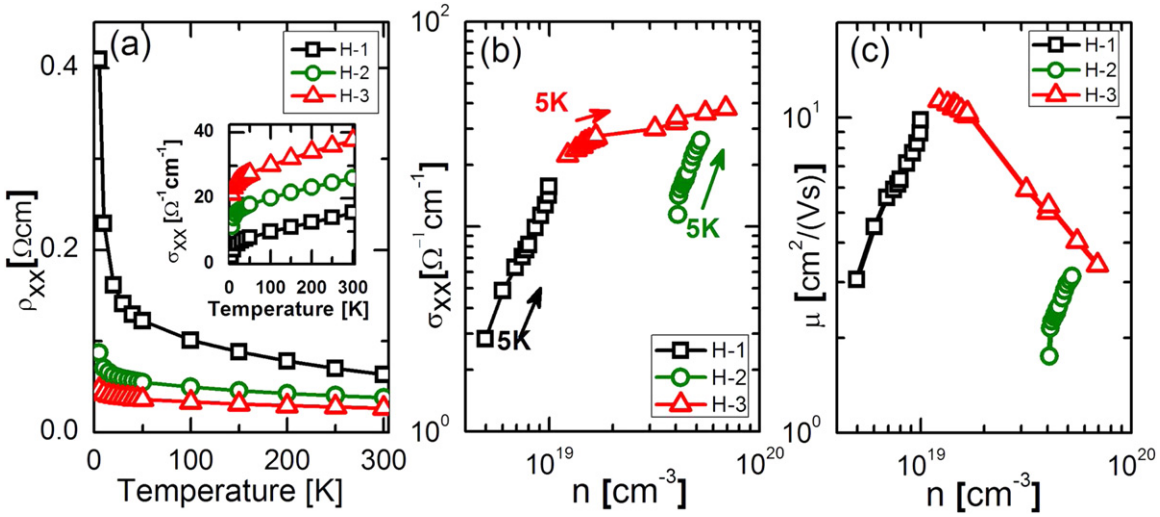

Figure 2. (a) Temperature dependences of longitudinal electrical resistivity (ρ_{xx}) of H-1, H-2 and H-3. The inset figure represents the enhancement of conductivity ($\sigma_{xx} = 1/\rho_{xx}$) with increasing temperature. (b) and (c) represent the n dependences of σ_{xx} and μ, respectively.

a metallic phase caused by the hydrogen injections. The thermally excited carrier from the localized state to the conduction band exhibits a temperature dependence of $\sim\exp(-E_a/k_BT)$, where E_a is the activation energy and k_B is Boltzmanns constant. For the temperature region between 150 K and 300 K, the E_a values for the H-1, H-2 and H-3 samples were observed to be 5.7, 3.3 and 2.7 meV, respectively. These small activation energies suggest that the H-related donor states are nearly degenerated on the conduction band minimum (CBM) [19]. In the low temperature region, the variable range hopping (VRH) has well described the transport for ZnO and Co-doped ZnO [20–22].

We examined the VRH characteristics of samples using the plot of ln (ρ_{xx}) versus $(T_0/T)^{-1/4}$, where T_0 is a characteristic temperature that is inversely proportional to the density of state (N_0) at the Fermi energy (E_F) in Motts conduction theory [23, 24]. Thus, the well-fitted linear slope below 50 K allows us to presume the existence of hopping transport in the low-temperature regime. However, compared with the reported T_0 for ZnO:H, the fitting results indicated a very small T_0. This result appears to be due to the hybridization between the H-s orbital and the Co-t_2 orbitals. The electronic structures of the H-1, H-2, and H-3 samples are discussed later in the first-principles calculation results.

Figures 2(b) and (c) illustrate the hydrogen effects on the n dependences of σ_{xx} and μ obtained through the Hall effect measurements. The analogous n-dependences in the σ_{xx}-n (figure 2(b)) and μ-n (figure 2(c)) graphs for the H-1 (black squares) and H-2 (green circles) samples are explained by the dominant scattering of electrons with charged interstitial H. However, σ_{xx} and μ of H-3 have different gradients from those of H-1 and H-2; in particular, the μ of the H-3 sample decreases with increasing n. In the H-1 and H-2 samples treated by relatively lower plasma powers, electrons dominantly scatter with the charged interstitial H near the surface, which results in an increase of μ with increasing n due to the Coulomb interaction. However, because the H in the H-3 sample is incorporated into the deeper layer of the ZnCoO

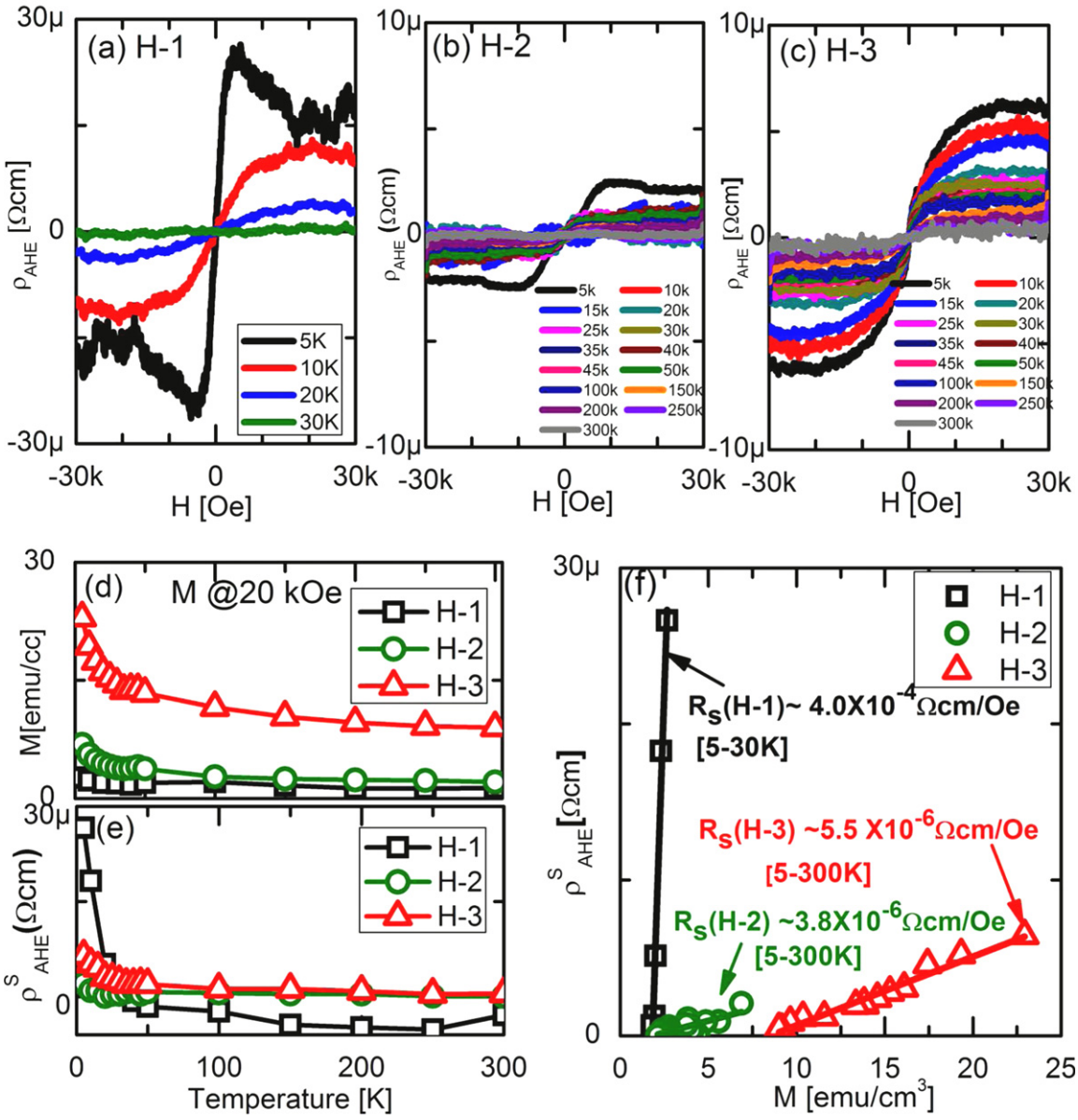

Figure 3. The temperature dependences of $\rho_{AHE}(H)$ for (a) H-1, (b) H-2 and (c) H-3. (d) Temperature dependence of magnetization (M) obtained at 20 kOe using a vibrating sample magnetometer (VSM). (e) Temperature dependence of saturated amplitude of ρ_{AHE} ($\rho^{s}_{AHE}(H)$). (f) The ρ^{s}_{AHE}-M relations of H-1 (between 5 K and 30 K) and H-2 and H-3 (between 5 K and 300 K). The solid lines represent the anomalous Hall coefficient, R_s, obtained by linear fitting.

thin film due to the higher plasma power, the contributions of a localized state driven by Co-H-Co complexes can be enhanced, which results in the decrease of μ with increasing n.

3.2. Anomalous Hall resistivity ($\rho_{AHE}(H)$)

Figure 3 shows that the increase of H drives H-induced localized states due to the formation of Co-H-Co complexes and that the asymmetric scattering between carriers and the states causes

the AHE. Generally, in Hall effect measurements for non-magnetic materials, the transverse voltage arises from a deflection charge caused by the Lorentz force effect (ordinary Hall effect) [25]. In this case, the resultant Hall resistivity (ρ_{xy}) is proportional to the magnetic field. However, in ferromagnetic materials, the ρ_{xy} additionally acquires the anomalous Hall resistivity (ρ_{AHE}), which is proportional to the magnetization (M) of the materials. Empirically, ρ_{xy} can be described as the sum of the ordinary and anomalous Hall resistivity, $\rho_{xy} = \rho_{OHE} + \rho_{\mathrm{AHE}} = R_o H + R_s \mu_0 M$, where R_o is the ordinary Hall coefficient, R_s is the anomalous Hall coefficient, and μ_0 is the vacuum permeability. Typically, the AHE is caused by the asymmetric scattering due to the spin-orbit coupling in the presence of spin-polarization.

Figures 3(a)–(c) show the magnetic field dependences of $\rho_{\mathrm{AHE}}(H)$ of the H-1, H-2 and H-3 samples in the temperature range between 5 and 300 K. From the measured $\rho_{xy}(H)$, we can obtain $\rho_{\mathrm{AHE}}(H)$ by subtracting the contribution of ρ_{OHE} above 20 kOe of magnetic field. In figure 3(a), the H-1 sample shows a relatively large $\rho_{\mathrm{AHE}}(H)$ at 5 K, decreases rapidly with increasing temperature and finally disappears at approximately 30 K. The amplitude ($\sim 27\ \mu\Omega cm$) of ρ_{AHE} at 5 K agrees with the reported value of the Al-doped ZnCoO sample, which exhibited an almost identical n as the H-1 sample at 5 K ($\sim 5 \times 10^{18}$ cm^{-3}) [26, 27]. The ρ^{s}_{AHE} of Al-doped ZnCoO also abruptly decreases with increasing n because of the decrease of spin polarization due to the spin-splitted conduction band [26–29]. Therefore, the large ρ_{AHE} of the H-1 sample is considered to be due to the spin-split conduction band as well as low n, which is similar to the case of Al-doped ZnCoO. In the H-2 sample (figure 3(b)), where the interstitial H enhances n, ρ_{AHE} deceases unlike that of the H-1 sample. It should be noted that the ρ_{AHE} of Al-doped ZnCoO abruptly decreases with decreasing (increasing) ρ_{xx} (n) [26, 27].

However, H-3 has a clear ρ_{AHE} and non-zero value even at room temperature (figure 3(c)), though its ρ_{xx} was much smaller than those of H-1 and H-2 (figure 1(a)). Figures 3(d) and (e) show the temperature dependencies of M and the fully saturated $\rho_{\mathrm{AHE}}(\rho^{s}_{\mathrm{AHE}})$ at 20 kOe. In particular, ρ^{s}_{AHE} and M of H-3 show a much similar temperature dependency, which clearly indicates a close link between electromagnetic transport and M. The linear behavior between ρ^{s}_{AHE} and M of H-3 is illustrated in figure 3(f), where R_s was determined to be $\sim 5.5 \times 10^{-6} \Omega$ cm Oe^{-1} over the entire temperature range. Considering the previous reports about hydrogen mediation [10–15, 17, 18], the ρ_{AHE} of H-3 is thought to originate from the asymmetric scattering of carriers by the Co-H-Co complex with parallel alignment of the Co-spin. We recently reported the effect of n on ZnCoO and ZnCoO:H via Al doping [30]; higher n did not contribute to greater ferromagnetism in ZnCoO:H. Furthermore, we have also reported that ferromagnetism can be markedly enhanced while maintaining the n [13]. Based on the relationship between the AHE and M, the Co-H-Co complex is one of strong candidates for main contribution to the change in the AHE. Therefore, it is obvious that the H-induced AHE of H-3 persisting up to 300 K has a different physical origin from that of H-1 observed only at low temperature. The small AHE signal for H-2 can be explained by the incorporation of interstitial H at the surface, which led to less formation of ferromagnetic Co-H-Co complexes and limited M to low values. In addition, the superparamagnetic contributions by ferromagnetic clusters (without a percolation process) cannot induce a large AHE, as observed in figure 3(c) [31].

3.3. Anomalous Hall conductivity ($\sigma_{AHE}(H)$)

Based on most theoretical predictions, the Hall conductivity ($\sigma_{xy} = \rho_{xy}/(\rho^2_{xx} + \rho^2_{xy})$) is considered to be an essential measurement in investigating the origin of AHE, where the Hall conductivity

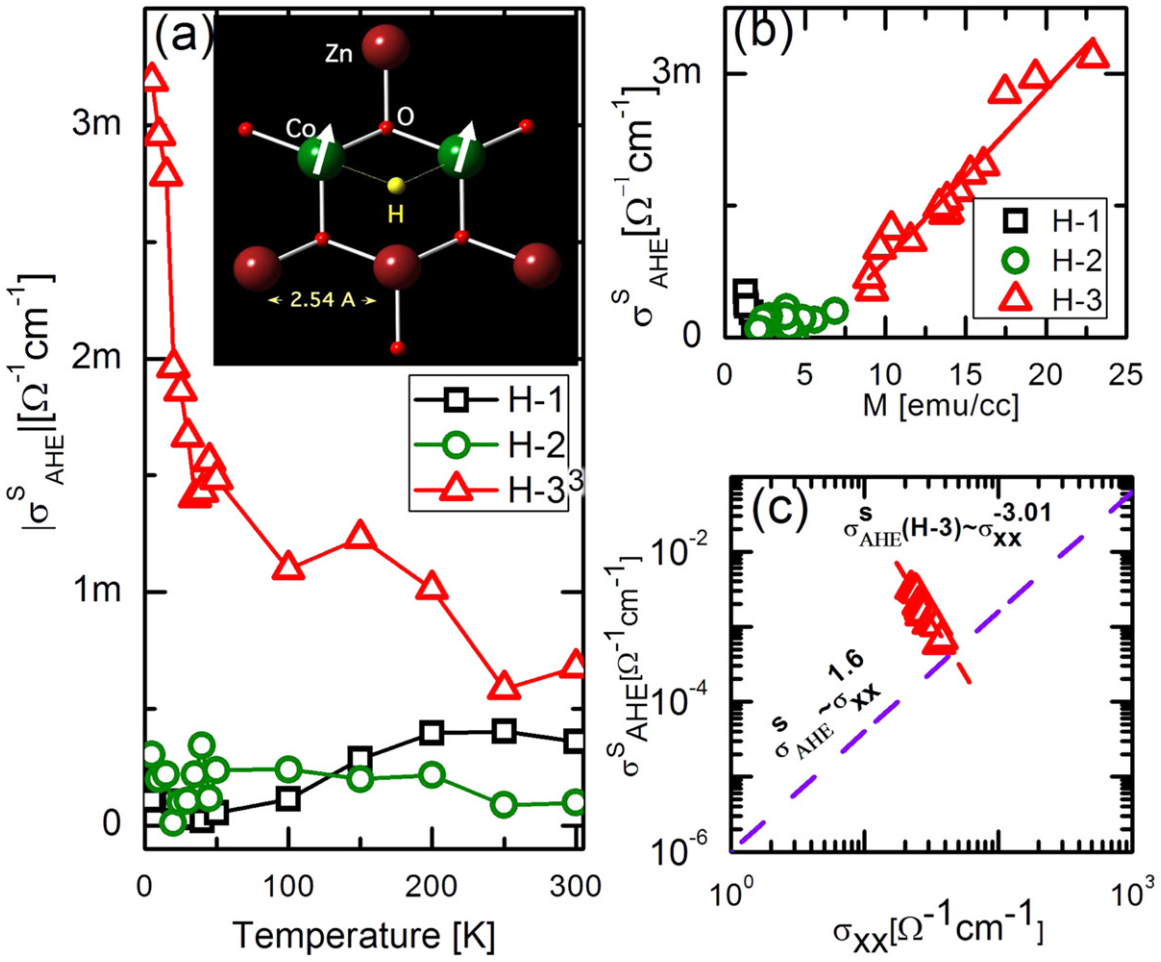

Figure 4. (a) Temperature dependences of the saturated $\sigma^{s}_{\mathrm{AHE}}$ for H-1, H-2 and H-3 (the inset figure represents the ferromagnetic Co-H-Co complex). (b) The magnetization dependence of $\sigma^{s}_{\mathrm{AHE}}$. The solid red line is obtained by linear fitting for H-3 from 5 K to 300 K. (c) The relation between σ_{xx} and $\sigma^{s}_{\mathrm{AHE}}$ of H-3 on a log-log scale (the violet dashed line represents the 1.6 scaling relation to guide the eye, and the red dashed line represents the fitting result of H-3).

σ_{xy} consists of σ_{OHE} and σ_{AHE}, and the strength of σ_{AHE} depends on both the contents of the carrier and the spin [7]. Figure 4(a) shows the temperature dependences of $\sigma^{s}_{\mathrm{AHE}}$ for all samples. H-1 only exhibits a small $\sigma^{s}_{\mathrm{AHE}}$ because of its low σ_{xx}. Although the interstitial H slightly enhanced the σ_{xx} value, H-2 still exhibited no remarkable enhancement of $\sigma^{s}_{\mathrm{AHE}}$.

However, H-3 exhibited a remarkable enhancement of $\sigma^{s}_{\mathrm{AHE}}$, especially at low temperatures, and a non-zero value of $\sigma^{s}_{\mathrm{AHE}}$ persisted up to room temperature. In particular, it should be noted that $\sigma^{s}_{\mathrm{AHE}}$ increased with decreasing temperature, though the σ_{xx} of H-3 clearly decreased with decreasing temperature (the inset of figure 1(a)). These results indicate that the $\sigma^{s}_{\mathrm{AHE}}$ of H-3 is strongly related to the formation of the Co-H-Co complex and its M (the inset figure of figure 4(a)). As observed in figure 4(b), the $\sigma^{s}_{\mathrm{AHE}}$ of H-3 also exhibits an almost linear proportionality to M, while the $\sigma^{s}_{\mathrm{AHE}}$ values of H-1 and H-2 are limited to low M and are not proportional to M. $\sigma^{s}_{\mathrm{AHE}}$ of H-3 at low temperatures has similar values to Co-doped TiO_2,

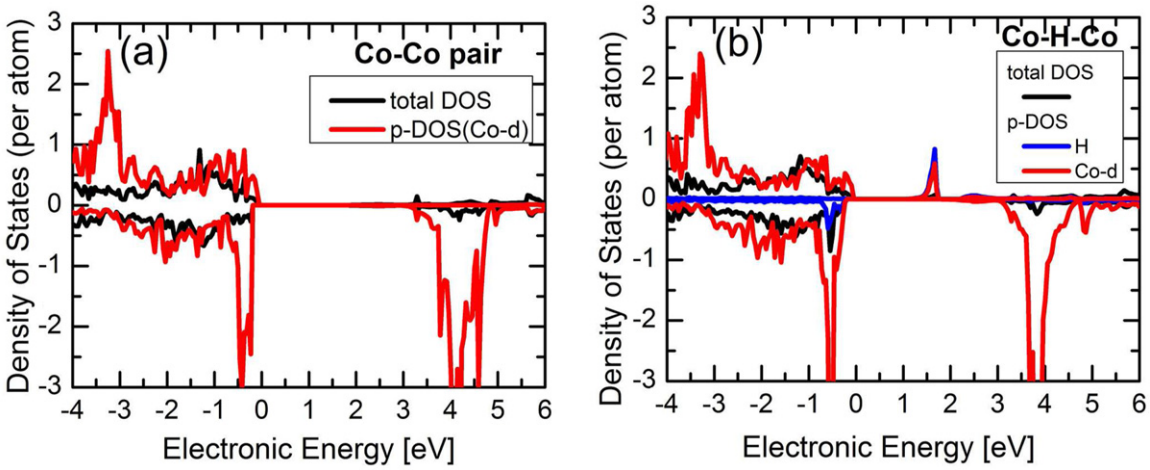

Figure 5. (a) The DOS and p-DOS for the Co-Co pair without H. (b) The calculated density of electronic states (DOS) for the H captured by the two nearest Co ions and the partial-DOS (p-DOS) from the H and Co-3d orbitals. The positive (negative) values describe the majority (minority) spin state.

and the value $\sim 0.7 \times 10^{-3}\Omega^{-1}$ cm^{-1} of H-3 observed at 300 K is comparable to the reported values enhanced by the gate-voltage at 300 K [7].

If σ_{AHE} has a scaling relation proportional to σ_{xx}, the AHE is ascribed to skew (asymmetric) scattering. If σ_{AHE} is proportional to σ_{xx}^2, the AHE is ascribed to the side-jump mechanism [32]. Recently, the characteristic scaling relation of $\sigma_{AHE} \propto \sigma_{xx}^{1.6}$ has been intensively investigated in many transition-metal-doped oxides as well as in GaAs-based magnetic semiconductors [1, 32–35]. Figure 4(c) shows the relations between σ_{xx} and $\sigma^{s}_{\mathrm{AHE}}$ on a log-log scale. The violet dashed line represents the 1.6 scaling relations to guide the eye. As observed in figure 4(c), though the σ_{xx} values of H-3 were spread too narrow to determine an exact scaling relation in the wide σ_{xx} range, we could estimate the scaling relation of $\sigma^{s}_{\mathrm{AHE}} \sim \sigma_{xx}^{-3.01}$ (red dashed line). Hence, we now see that the origin of the AHE of H-3 is different from that of the other magnetic semiconductors, showing the 1.6 scaling relation because the observed H-induced AHE originates from the asymmetric scattering of carrier hopping between the localized states driven by ferromagnetic Co-H-Co complexes.

3.4. Localized state driven by hybridization between the H–1s and Co-t_2 orbitals

We examined the electronic structure of ZnCoO:H using first-principles calculations, which were performed using the projector augmented wave (PAW) method [36] of the Vienna *ab initio* simulation package (VASP) [37].

The Perdew–Burke–Ernzerhof exchange-correlation functional (PBE) [38] approach utilizing the generalized gradient approximation (GGA) scheme was employed, and the local spin density approximation (LSDA)+U method was used to compensate for the Coulomb interaction in the localized semi-core Zn-3d and Co-3d orbitals [39]. We used U = 5 eV. The state of the capture of H between two nearest $\mathrm{Co_{Zn}}$, which is compared with the state without H capture and the density of electronic states, is shown in figures 5(b) and (a), respectively. A previous study indicated that H can be strongly captured between two Co ions and that the Co-

spin can be parallelly aligned by the H capture, which was suggested to lead to the ferromagnetism of ZnCoO [10].

In transition metal-doped ZnO, the competition between the ferromagnetic double-exchange interaction and the antiferromagnetic superexchange interaction has been considered [40, 41]. It has also been reported that the ferromagnetic state is stabilized by electron doping in Co-doped ZnO [40, 41]. Electrically, H increases n by acting as a shallow donor. Based on the Zeners double-exchange mechanism, the enhanced n contributes to ferromagnetism. However, in ZnCoO:H, H serves as an additional strong magnetic channel for short-range ferromagnetic spin–spin interactions between Co dimers; this interaction dominates the expected contribution from the double-exchange interaction at room temperature [10]. In ZnCoO:H, the Zeners double-exchange mechanism is expected, although it does not lead to room temperature ferromagnetism [10]. In the ferromagnetic state, which can be mediated by H, the free carriers at the conduction band edge can be partially spin-polarized by the spin-carrier double-exchange interaction.

In figures 5(a) and (b), a remarkable finding is that the localized state driven by the Co-H-Co center is generated at the CBM. The localized state originates from the hybridization between the H-s orbital and the Co-t_2 orbitals, which indicates that the electron carrier mobility can be significantly reduced by the hydrogen contamination and that the electron carrier can be transported by the hopping mechanism between the localized states. The electron carrier is not provided by the Co-H-Co center; however, it can be generated by the interstitial H in the presence of a high concentration of H. These results indicate that the observed H-induced AHE originates from the asymmetric scattering of carrier hopping between the localized states formed by a hybridization between the H-s orbital and Co-t_2 orbitals, which is driven by the Co-H-Co complex persisting ferromagnetic spin ordering up to room temperature.

4. Conclusion

In summary, we report the H-induced electrical transport characteristics and the unique AHE attributed to a ferromagnetic spin ordering of Co-H-Co complexes in Co-doped ZnO thin films. In H-1 with the low H-injection condition, the interstitial H causes a significant decrease in $\rho_{xx}$with the decreasing AHE originating from the spin-split conduction band, which is similar to the contributions of other n-type dopants in ZnCoO. However, as the injected H forms ferromagnetic Co-H-Co complexes with a higher H-injection process, the characteristic AHE increases. Furthermore, the H-induced ferromagnetic response of the carrier persists up to room temperature while being proportional to the amplitude of M due to the ferromagnetic complexes. The origin of the AHE of H-induced ferromagnetism is different from that of other magnetic semiconductors because it originates from the asymmetric scattering of carrier hopping between the localized states driven by ferromagnetic Co-H-Co complexes. The theoretical calculation results indicate that the localized state driven by the Co-H-Co center is generated at the CBM, which supports very well the idea that the AHE in a hydrogen-mediated system is attributed to the asymmetric scattering of carrier hopping between the localized states driven by ferromagnetic Co-H-Co complexes.

Acknowledgments

This research was supported by the Converging Research Center Program through the Ministry of Science, ICT and Future Planning, Korea (MSIP) (2013K000310) and by Basic Science Research Program through the National Research Foundation of Korea (NRF) funded by the Ministry of Education, Science and Technology (2011–0010789).

References

[1] Toyosaki H, Fukumura T, Yamada Y, Nakajima K, Chikyow T, Hasegawa T, Koinuma H and Kawasaki M 2004 *Nat. Mater.* **3** 221
[2] Ohno H, Chiba D, Matsukura F, Omiya T, Abe E, Dietl T, Ohno Y and Ontani K 2000 *Nature* **408** 944
[3] Chiba D, Yamanouchi M, Matsukara F and Ohno H 2003 *Science* **301** 943
[4] Koshihara S, Oiwa A, Hirasawa M, Katsumoto S, Iye Y, Urano C, Takagi H and Munekata H 1997 *Phys. Rev. Lett.* **78** 4617
[5] Dietl T, Ohno H, Matsukura F, Cibert J and Ferrand D 2000 *Science* **287** 1019
[6] Matsumoto Y, Murakami M, Shono T, Hasegawa T, Fukumura T, Kawasaki M, Ahmet P, Chikyow T, Koshihara S and Koinuma H 2001 *Science* **291** 854
[7] Yamada Y, Ueno K, Fukumura T, Yuan H T, Shimotani H, Iwasa Y, Gu L, Tsukimoto S, Ikuhara Y and Kawasaki M 2011 *Science* **332** 1065
[8] Katayama-Yoshida H, Sato K, Fukushima T, Toyoda M, Kizaki H, Dinh V A and Dederichs P H 2007 *J. Magn. Magn. Mater.* **310** 2070
[9] Sato K, Fukushima T and Katayama-Yoshida H 2007 *Japan. J. Appl. Phys.* **46** L682
[10] Park C H and Chadi D J 2005 *Phys. Rev. Lett.* **94** 127204
[11] Cho Y C *et al* 2009 *Appl. Phys. Lett.* **95** 172514
[12] Lee S, Cho Y C, Kim S J, Cho C R, Jeong S-Y, Kim S J, Kim J P, Choi Y N and Sur J M 2009 *Appl. Phys. Lett.* **94** 212507
[13] Cho Y C, Lee S, Nahm H H, Kim S J, Park C H, Lee S Y, Kim S-K, Cho C R, Koinuma H and Jeong S-Y 2012 *Appl. Phys. Lett.* **100** 112403
[14] Kim S J, Lee S, Cho Y C, Choi Y N, Park S, Jeong I K, Kuroiwa Y, Moriyoshi C and Jeong S-Y 2010 *Phys. Rev.* B **81** 212408
[15] Lee S *et al* 2014 *Appl. Phys. Lett.* **104** 052405
[16] Toyoda M, Akai H, Sato K and Katayama-Yoshida H 2006 *Phys. Status Solidi* c **3** 4155
[17] Kim S J *et al* 2012 *J. Phys. Chem.* C **116** 12196
[18] Lee S, Kim B S, Cho Y C, Shin J M, Seo S W, Cho C R, Takeuchi I and Jeong S-Y 2013 *Curr. Appl. Phys.* **13** 2005
[19] Li Y J, Kaspar T C, Droubay T C, Zhu Z, Shutthanandan V, Nachimuthu P and Chambers S A 2008 *Appl. Phys. Lett.* **92** 152105
[20] Singh A, Chaudhary S and Pandya D K 2013 *Appl. Phys. Lett.* **102** 172106
[21] Behan A J, Mokhtari A, Blythe H J, Score D, Xu X H, Neal J R, Fox A M and Gehring G A 2008 *Phys. Rev. Lett.* **100** 047206
[22] Chou H, Lin C P, Hsu H S and Sun S J 2010 *Appl. Phys. Lett.* **96** 092503
[23] Li Y J, Kaspar T C, Droubay T C, Joly A G, Nachimuthu P, Zhu Z, Shutthanandan V and Chambers S A 2008 *J. Appl. Phys.* **104** 053711
[24] Mott N F and Davis E A 1979 *Electronic Process in Non-crystalline Materials* 2nd edn (Oxford: Clarendon)
[25] Hall E H 1880 *Phil. Mag.* **10** 301
Hall E H 1881 *Phil. Mag.* **12** 157

[26] Xu Q, Hartmann L, Schmidt H, Hochmuth H, Lorenz M, Schmidt-Grund R, Sturm C, Spemann D and Grundmann M 2006 *Phys. Rev.* B **73** 205342
[27] Xu Q, Hartmann L, Schmidt H, Hochmuth H, Lorenz M, Schmidt-Grund R, Sturm C, Spemann D and Grundmann M 2007 *J. Appl. Phys.* **101** 063918
[28] Andrearczyk T, Jaroszyński J, Grabecki G, Dietl T, Fukumura T and Kawasaki M 2005 *Phys. Rev.* B **72** 121309 R
[29] Tian Y, Li Y and Wu T 2011 *Appl. Phys. Lett.* **99** 222503
[30] Park J H, Lee S, Kim B S, Kim W K, Cho Y C, Oh M W, Cho C R and Jeong S Y 2014 *Appl. Phys. Lett.* **104** 052412
[31] Zhang S X *et al* 2007 *Phys. Rev.* B **76** 085323
[32] Nagaosa N, Sinova J, Onoda S, MacDonald A H and Ong N P 2010 *Rev. Mod. Phys.* **82** 1539
[33] Chiba D, Werpachowska A, Endo M, Nishitani Y, Matsukura F, Dietl T and Ohno H 2010 *Phys. Rev. Lett.* **104** 106601
[34] Ueno K, Fukumura T, Toyosaki H, Nakano M and Kawasaki M 2007 *Appl. Phys. Lett.* **90** 072103
[35] Venkateshvaran D, Kaiser W, Boger A, Althammer M, Rao M S R, Goennenwein S T B, Opel M and Gross R 2008 *Phys. Rev.* B **78** 092405
[36] Blöchl P E 1994 *Phys. Rev.* B **50** 17953
[37] Kresse G and Furthmuller J 1996 *Phys. Rev.* B **54** 11169
[38] Perdew J P, Burke K and Ernzerhof M 1996 *Phys. Rev. Lett.* **77** 3865
[39] Anisimov V I, Zaanen J and Andersen O K 1991 *Phys. Rev.* B **44** 943
[40] Sato K and Katayama-Yoshida H 2000 *Japan. J. Appl. Phys.* **39** L555
[41] Sato K *et al* 2010 *Rev. Mod. Phys.* **82** 1633